PHYSICAL REVIEW B VOLUME 18, NUMBER 7 1 OCTOBER 1978

# Pressure dependence of magnetic excitations in SmS

D. B. McWhan
*Bell Laboratories, Murray Hill, New York 07974*

S. M. Shapiro and J. Eckert
*Brookhaven National Laboratory, Upton, New York 11973*

H. A. Mook
*Oak Ridge National Laboratory,* Oak Ridge, Tennessee 37830*

R. J. Birgeneau
*Department of Physics and Center for Materials Science and Engineering, Massachusetts Institute of Technology, Cambridge, Massachusetts 02139*

(Received 5 June 1978)

Inelastic-neutron-scattering studies using triple-axis and time-of-flight techniques have been made in the low- and high-pressure phases of a polycrystalline sample of $^{154}$SmS. There is no observable change in the energy or width of the $^7F_0$-$^7F_1$ excitation of the $4f^6$ configuration between ambient pressure and 0.6 GPa. In the mixed-valence phase at high pressure, there is no evidence for well-localized excitations from either the $^7F_0$-$^7F_1$ ($4f^6$) or the $\Gamma_7$-$\Gamma_8$ ($^6H_{5/2}$, $4f^5$) configurations. These results suggest that the mixed-valence phase is homogeneous. Lattice-parameter measurements versus pressure at 85 and 298 K show no evidence for pretransitional softening and establish that the phase diagram in the $P$-$T$ plane is reentrant. From the phase diagram and earlier heat-capacity measurements, the electronic entropy in the mixed-valence phase is estimated to saturate at $\simeq 2R$ with increasing temperature.

## I. INTRODUCTION

There are a number of first-order phase transitions in which there is no change in symmetry. These transitions are electronic in origin and involve the merging of different energy bands as in SmS,[1] Ce,[2] and Cs,[3] or changes from band to localized states as in $(V_{1-x}Cr_x)_2O_3$,[4] for $Ti_4O_7$.[5] A common feature of the first-order transitions in Cs, Ce, and SmS is that they do not go completely $s \rightarrow d$ or $f^n \rightarrow f^{n-1}d$, but instead, the high-pressure phases appear to have electronic structures which are between the two limits.[6] In SmS the transition at 0.65 GPa (1 GPa = 10 kbar) is to a mixed-valence phase which is $0.2(f^6) + 0.8(f^5d)$.[7]

The physical properties of the mixed-valence phase of SmS suggest that the $f$ electrons, which obey atomic selection rules, and the $s$-$d$ electrons coexist at the Fermi surface. The specific heat has a very large linear term ($\gamma = 145$ mJK$^{-2}$ mole$^{-1}$),[8] and the magnetic susceptibility saturates at low temperatures[9] at a value suggestive of the enhanced Pauli susceptibility of a narrow band.[10] As there will be either five or six $f$ electrons on a given Sm ion at any given instant, it is not clear why the magnetic ground state of the $f^5$ configuration ($^6H_{5/2}$) does not lead to a divergence of the susceptibility. Depending on the rate at which the two configurations fluctuate, the ground state of the mixed-valence phase may be homogeneous or inhomogeneous. $Ti_4O_7$ is an inhomogeneous mixed-valence compound with the $Ti^{3+}(3d^1)$ and $Ti^{4+}(3d^0)$ ions spatially ordered, with a resulting energy gap for electron transport.[5] On the other hand SmS, in the high-pressure phase, is believed to be an example of a homogeneous mixed-valence phase because Mössbauer measurements show a single absorption with an isomer shift which is 70% of the way from that expected for a $4f^6$ configuration to that expected for a $4f^5$ configuration.[11]

Inelastic neutron scattering is a powerful tool for studying the atomic excitations of the $4f$ electrons in rare-earth metals and compounds. A large body of data on crystal-field levels and the energy levels within the atomic $J$ manifolds has been obtained.[12] A detailed study of the temperature dependence of the dispersion relation for the $^7F_0$-$^7F_1$ excitation of SmS at 1 atm is in good agreement with the mean-field random-phase-approximation theory for the dynamics of the idealized singlet-triplet model.[13] The $^7F_0$-$^7F_1$ separation ($420 \pm 2$ K) is close to the free-ion value of 422 K, and the exchange interactions are characteristic of a magnetic semiconductor. In a preliminary study, the $^7F_0$-$^7F_1$ excitation in SmS seemed to disappear on going through the phase transition to the mixed-valence phase, but the signal-to-noise ratio was poor.[14] In this paper, we present a detailed study of the $^7F_0$-$^7F_1$ excitation and the lattice parameter as a function of pressure. No sub-

 

stantial softening of the lattice is evident in the lattice-parameter measurements, and no observable broadening of the $^7F_0$-$^7F_1$ excitation is observed, right up to the transition pressure. The lattice parameter measurements, which were made in a He-gas pressure cell, confirm the reentrant nature of the phase boundary in pure SmS. In the mixed-valence phase no evidence is found for well-localized excitations from either the $^7F_0$-$^7F_1$ transition of the $4f^6$ configuration or the $\Gamma_7$-$\Gamma_8$ crystal-field transition of the $4f^5$ ($^3H_{5/2}$) configuration. The detailed experimental results are presented in Sec. II, and their implications with regard to the nature of the ground state of mixed-valence compounds and with regard to the phase transition to the mixed-valence phase are discussed in Sec. III.

## II. EXPERIMENTAL

Inelastic-neutron-scattering measurements at high pressure have been performed both on a triple-axis spectrometer at the Brookhaven National Laboratory high flux beam reactor and on a time-of-flight spectrometer at the Oak Ridge high flux isotope reactor. A polycrystalline sample of SmS made from the isotope $^{154}$Sm was used because natural Sm has a prohibitively large absorption cross section for thermal neutrons. The preliminary measurements of the $^7F_0$-$^7F_1$ excitation were hampered by the low signal-to-noise ratio resulting from the small sample size.[14] To overcome this problem a larger (~7 g) sample of $^{154}$SmS was obtained by combining the sample made for the measurements of the induced magnetic form factor[15] with the sample used in the preliminary study. The measurements at high pressure were made in one of three different devices, a helium-gas apparatus, a piston-cylinder device made of an aluminum alloy or one made of beryllium-copper. The helium-gas apparatus has been described previously[16] and consisted of an aluminum alloy (7075-T6) cell mounted in a cryostat with steel capillary tubing transferring the helium gas from an intensifier outside to the pressure cell. One of the piston-cylinder devices was also made from the Al 7075 alloy and used a fluorocarbon (Fluorinert FC-75, manufactured by the 3*M* Company, St. Paul, Minn.) as the pressure transmitting medium. This cell was mounted in a high-pressure cryostat, which is capable of delivering 20 tons to the pressure die, which in turn is cooled by a closed cycle helium refrigerator.[17] The last cell, made from beryllium copper (Berylco 25) was a clamp device and was used for the magnetic form factor measurements.[15] The pressure could be varied *in situ* in the first two devices, but the clamp device had to be demounted in order to change the pressure. There was an additional change in pressure on cooling in the beryllium-copper apparatus. These devices had maximum working pressures of 0.8–1.0 GPa (1 GPa = 10 kbar), and in each one it was not possible to obtain more than 80% conversion into the high-pressure phase. Presumably part of the sample is off-stoichiometry or contains impurities such as oxygen which result in a large range of transition pressures.

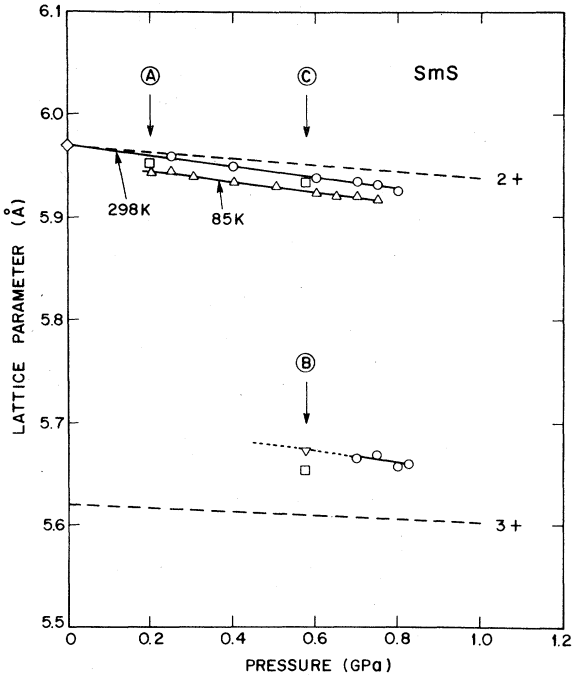


FIG. 1. Lattice parameter vs pressure at 85 K (triangles and squares) and 298 K (circles, diamonds, and inverted triangle). The dashed lines represent the expected lattice parameters of SmS with $4f^6$($Sm^{2+}$) and $4f^55d$ ($Sm^{3+}$) configurations. The letters A, B, and C identify the squares which give the lattice parameters and pressures associated with the corresponding curves in Fig. 3.

The lattice parameters as a function of pressure at both $T = 298$ K and 85 K are shown in Fig. 1. The measurements were made in the helium-gas apparatus on a triple-axis spectrometer with a neutron energy of 14.8 meV. Pyrolytic graphite crystals were used as monochromator, analyzer, and filter to eliminate higher-order contamination. A 20-min horizontal collimation was used either before or after the monochromator and 40-min collimation in the remainder of the spectrometer. The fraction of the sample in the high-pressure phase was determined by comparing the integrated intensity of the {200} reflections of each phase. A comparison of the isothermal compres-

sions at 298 and 85 K indicates that the transition pressure under hydrostatic conditions is ~0.1 GPa higher at the lower temperature. The dashed lines represent the lattice parameters versus pressure expected, on the basis of the systematics of rare-earth chalcogenides,[7] for SmS with either a $4f^6$ or $4f^5$ configuration. There is only a small increase in compressibility for the low-pressure phase and no evidence for an enhanced softening near the transition.

In conjunction with the measurements of the induced magnetic form factor,[15] inelastic-neutron-scattering measurements were made at 15 K in the beryllium-copper clamp device both in the low-pressure phase and at high pressure with the sample ~80% in the collapsed phase. A magnetically pulsed time-of-flight spectrometer was used with an incident energy of 70 meV.[18] The results at $Q = 1.8$ Å$^{-1}$; normalized to the same monitor count and with the background subtracted, are shown in Fig. 2. The transmission of the cell and the integrated intensity of the Bragg peaks were monitored in order to minimize differences between the two sets of data which might result from demounting the cell. The spectrometer resolution was ~5 meV. The integrated intensity was studied as a function of $Q$ to establish that it falls off in a manner consistent with the magnetic form factor. The disappearance of the $J = 0 \rightarrow 1$ excitation at 36 meV in the collapsed phase is clearly seen in Fig. 2. Although the intensity of the Bragg peaks indicates that 20% of the sample is in the low-pressure phase, there is no obvious remnant of the $J = 0 \rightarrow 1$ excitation in the high-pressure data.

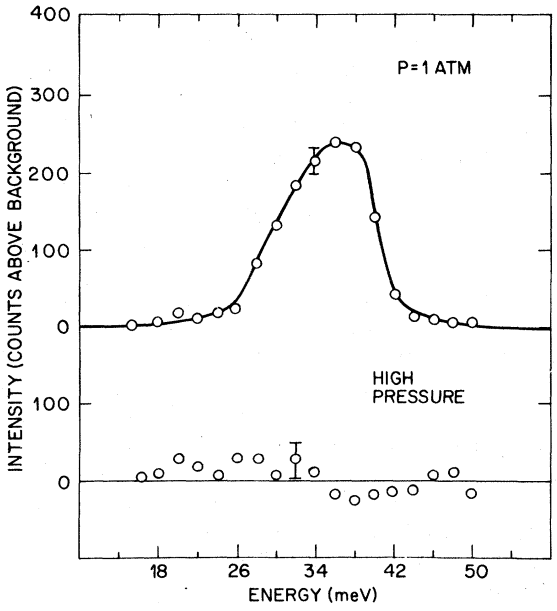


FIG. 2. Intensity vs energy in the region of the $^7F_0$-$^7F_1$ excitation at 1 atm and at high pressure. The data were obtained using time-of-flight techniques in a beryllium-copper cell.

The inelastic-neutron-scattering measurements using the aluminum alloy cell were made on a triple-axis spectrometer under the conditions described above for the lattice-parameter measurements. Constant-$Q$ energy scans were performed with a fixed analyzer energy of 14.8 meV. The data were collected at a temperature of 80–100 K at the points marked A, B, and C in Fig. 1. The sample was warmed to above 273 K before varying the pressure, and the apparatus was temperature cycled at constant applied load to minimize strain effects as the Fluorinert turned glassy on cooling. The pressure calibration was based on scaling the measured applied load at the transition to 0.65 GPa. The sequence of data collection was as follows: First the pressure was increased to ~0.2 GPa in the low-pressure phase (A). Second, by taking advantage of the large hysteresis in the first-order transition, the pressure was cycled as high as possible and then was released to ~0.6 GPa in the collapsed phase (B). Finally, the pressure was released, then cycled up to ~0.6 GPa in the low-pressure phase (C). In this way it was possible to determine if any precursor effects were observable in the $J = 0$–$1$ excitation and to compare directly the magnetic scattering in the low- and high-pressure phases under the same conditions of pressure and temperature. The results are shown in Fig. 3 where the zero of each set of data has been displaced for clarity. The solid lines in Fig. 3 are a guide to the eye for the background. The same background line is used for each of the top three curves for which $Q = 2.65$ Å$^{-1}$ and similarly for the bottom two curves for which $Q = 4$ Å$^{-1}$. The line through the excitation at 36 meV in the top curve is a least-squares fit assuming a Gaussian line shape. The resulting full width at half maximum is 3.9 meV which is to be compared with the calculated resolution function width of 3.2 meV. The solid lines between 30 and 40 meV in the other curves were obtained by scaling the Gaussian for the 0.2 GPa curve by the fraction of the sample in the low-pressure phase (obtained from the intensities of the 200 reflections of the low- and high-pressure phase) and the measured magnetic form factor. The fact that the intensity of the excitation in the low-pressure phase decreases with increasing $Q$ confirms that it is magnetic in origin. The data in the bottom curve are slightly above the calculated line between 32 and 38 meV, but at large $Q$ the contributions from phonons are not insignificant as evidenced by the increased slope of the background. The optical-phonon modes of SmS are

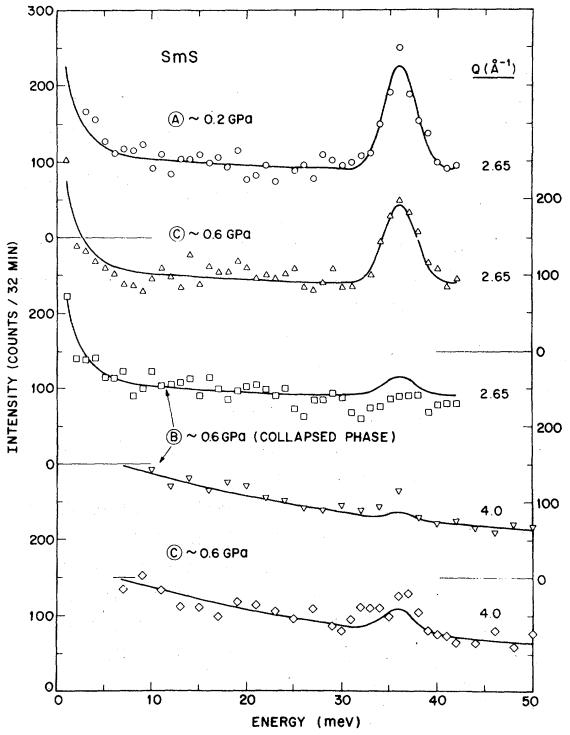


FIG. 3. Intensity vs energy for the pressures indicated in Fig. 1 and at $Q = 2.65$ Å$^{-1}$ (top 3 curves) and 4.0 Å$^{-1}$ (bottom 2 curves). The solid lines are guides to the eye through the background and a Gaussian fit to the $^7F_0$-$^7F_1$ excitation in curve A is scaled down as described in the text in the other curves. There is no evidence for either the $^7F_0$-$^7F_1$ excitation of a $4f^6$ or a $\Gamma_7$-$\Gamma_8$ excitation of a $4f^5$ configuration at 36 and 13 meV, respectively, in the collapsed phase (curves 3 and 4).

believed to lie in this energy range. A comparison of the top two curves shows no evidence for observable broadening of the excitation right up to the transition pressure. The third curve shows no evidence for a sharp $J = 0$–1 excitation or for a sharp $\Gamma_7$-$\Gamma_8$ crystal-field excitation in the collapsed phase. As observed in the time-of-flight measurements (Fig. 2) the $J = 0$–1 excitation for the remaining 20% of the low-pressure phase is also not evident.

## III. DISCUSSION

There are two aspects to the problem of mixed-valence compounds. First is the understanding on a microscopic level of the nature of the ground state of the system. Second is the understanding of the phase transition into the mixed-valence phase. On the phenomenological level, as pointed out by Varma,[10] the experimental results for the mixed-valence phase are characteristic of a two-component Fermi liquid. One liquid is very heavy with a degeneracy temperature of less than 0.1 eV and is composed principally of the $4f$ electrons. The second liquid is composed principally of the $s$-$d$ electrons, and the two liquids are coupled, to a first approximation, by the $f$-$d$ transfer integral which leads to a strong hybridization of the ground-state wave function. However, as the $4f$ electron liquid is highly correlated, it is difficult to give a microscopic description of these hybridized, correlated band orbitals. The inelastic-neutron-scattering results are discussed below in terms of the local atomic excitations and the $f$-$d$ hybridization, and the results are compared with neutron scattering studies on other mixed-valence materials. In the second part of the discussion the available data on the phase boundary in the pressure-temperature plane and the low-temperature heat-capacity results are combined to obtain an estimate of the temperature dependence of the electronic entropy in the mixed-valence phase.

### A. Ground state of the mixed-valence phase

At 1 atm the $4f$ electrons of SmS are well characterized by an ionic model in which the degeneracy of the ground-state $J$ multiplet is lifted by spin-orbit coupling to give the levels $^7F_J$ with $J = 0, 1, \ldots, 6$. The top two curves in Fig. 3 clearly show that this ionic description of the low-pressure phase of SmS is valid right up to the phase transition. There is no observable broadening of the $^7F_0$-$^7F_1$ excitation between 0.2 and 0.6 GPa. (The decrease in intensity is entirely accounted for by the partial transformation of the sample into the high-pressure phase.)

In the high-pressure phase the lattice parameter measurements suggest that in an ionic model there would be a mixture of $0.2\,f^6$ Sm ions and $0.8\,f^5$ Sm ions. A $4f^5$ configuration would have a $^6H_{5/2}$ ground state which would be split into a $\Gamma_7$ doublet and a $\Gamma_8$ quartet by the cubic crystal field of the NaCl structure. The possible energy of the $\Gamma_7$-$\Gamma_8$ excitation can be estimated from the observed value of the crystal field parameter $A_4\langle r^4\rangle = 13.3$ meV of PrS,[19] if an $R^5$ dependence is assumed for interatomic distance. This gives $A_4\langle r^4\rangle \approx 14.3$ meV and $E(\Gamma_8)$-$E(\Gamma_7) \approx 12.9$ meV (150 K) for the $4f^5$ configuration of a hypothetical high-pressure phase of SmS. It should be emphasized, however, that the crystal-field splitting in the mixed-valence state may be fundamentally different from the normal state so that the above estimate should only be used as a guide.

The relative intensities of the $^7F_0$-$^7F_1$ and the $\Gamma_7$-$\Gamma_8$ excitations can be calculated in the dipole approximation. Within a given $J$ multiplet and in the limit of small momentum transfers, the neu-

tron scattering cross section for an assemblage of $N$ noninteracting ions is[19,20]

$$\frac{d^2\sigma}{d\Omega\, d\omega} = N\left(\frac{1.91e^2}{2mc^2}\right)[f(\vec{Q})]^2 \frac{k_f}{k_i} \times \sum \rho_n g_J^2 |\langle n|\vec{J}_\perp|m\rangle|^2 \delta\left(\frac{\epsilon_n - \epsilon_m}{h} - \omega\right),$$

where $|n\rangle$ and $|m\rangle$ are states belonging to a given $J$ multiplet and $\vec{J}_\perp$ is the component of the total angular momentum operator perpendicular to the scattering vector $\vec{Q}$; $g_J$ is the Landé splitting factor; $\rho_n$ the population of the $n$th state and $f(\vec{Q})$ is the magnetic form factor which has been measured as a function of pressure for SmS,[15] and $k_f/k_i$ is the ratio of the final and initial momenta of the scattered neutron. For the $\Gamma_7$-$\Gamma_8$ transition the appropriate factors at $T = 85$ K with the analyzer energy fixed at 14.8 meV are $|\langle\Gamma_7|\vec{J}_\perp|\Gamma_8\rangle|^2 = 8.89$,[21] $g_J = \frac{2}{7}$, $\rho(\Gamma_7) = 0.78$, and $k_f/k_i = 0.713$. This gives

$$\frac{d^2\sigma}{d\Omega\, d\omega} = 0.40C[f(\vec{Q})]^2 \delta\left(\frac{E(\Gamma_7 - \Gamma_8)}{h} - \omega\right),$$

where $C = N(1.91e^2/2m_c^2)^2$. The cross section for the $4f^6$ $^7F_0$-$^7F_1$ transition is obtained by replacing the summation above by $2\rho(^7F_0)\,|\langle^7F_0|\vec{L} + 2\vec{S}|\,^7F_1\rangle|^2$.[13] This gives

$$\frac{d^2\sigma}{d\Omega\, d\omega} = 4.22C[f(\vec{Q})]^2 \delta\left(\frac{E(J=0-1)}{h} - \omega\right).$$

Finally, it is necessary to consider the paramagnetic case in the quasielastic limit in which we integrate overall energies. In this case the total scattering cross section for a band of $4f^5$ electrons is

$$\frac{d\sigma}{d\Omega} = \tfrac{2}{3} C g_J^2 J(J+1)[f(\vec{Q})]^2 = 0.48C.$$

In an ionic model if the integrated intensity of the $^7F_0$-$^7F_1$ excitation at 0.2 GPa in Fig. 3 is taken to be ~530 counts/32 min, then in the high-pressure phase the relative integrated intensities of the $\Gamma_7$-$\Gamma_8$ and $^7F_0$-$^7F_1$ excitations should be 30 and 190, respectively. (For the $J = 0$–1 excitation this includes the 20% of the sample remaining in the low-pressure phase plus the 20% of the high-pressure phase which would be $4f^6$.) Taking into account resolution corrections the peak intensities would be ~30 and ~50 counts, respectively, at ~13 and ~36 meV. There is no evidence for either of these excitations in the third curve from the top in Fig. 3. There is also no evidence for the $J = 0$–1 excitation in the 20% of the sample which is untransformed. A possible explanation for this is that the change in stoichiometry or chemical composition which causes the increase in the transition pressure for part of the sample also leads to larger exchange interactions and hence broadens the excitation. It is known from studies of the Eu chalcogenides that the exchange is very sensitive to impurities.[22] It is clear that there has been a dramatic change in the electronic structure on an atomic scale, but it is not known if the crystal-field splitting is substantially different from the expected value or if the change is due to fluctuations. If the ions are fluctuating then the excitations would be broadened and lost in the background. Similarly if the $f^5$ electrons were broadened into a band then the resulting Lorentzian centered around $E = 0$ with a total integrated intensity of 60 counts/32 min would be difficult to observe.

The absence of a sharp excitation corresponding to ionic $4f^5$ and $4f^6$ configurations in the mixed-valence phase is consistent with neutron scattering results on other mixed-valence compounds. In $CePd_3$ a quasielastic line with a Lorentzian shape has been observed.[23] This implies that the dynamic susceptibility has the relaxational form:

$$\chi''(\vec{Q}, \omega) = C\Gamma\omega/(\Gamma^2 + \omega^2),$$

where $C$ is a normalization constant and $\hbar\Gamma$ is a measure of the magnetization fluctuation energy. In $CePd_3$ this energy is $\hbar\Gamma \approx 19$ meV and the total cross section suggests a mixed valence of 0.5 $4f$ electron per formula unit. In $Ce_{0.74}Th_{0.26}$ there is a first-order transition at 150 K at which the effective number of $4f$ electrons jumps from 0.7 to 0.6 with decreasing temperature. This jump is accompanied by a dramatic increase in $\hbar\Gamma$ from 24 to 72 meV.[24] By analogy with these systems the spin dynamics in SmS may also change from localized to itinerant at the phase transition.

Finally it is of interest to point out the apparent difference between the integral and the mixed-valence state as probed by inelastic neutron scattering and elastic polarized neutron scattering. There is a large change in the magnetic excitations in the former, but there is no observable change in the induced magnetic form factor.[15] The magnetic contribution to the latter scattering simply scales with the static susceptibility. The absence of the induced magnetic form factor anticipated for an ionic $4f^5$ configuration has been rationalized on the basis of renormalizing the susceptibility by an artificial interconfiguration fluctuation temperature $\Delta$, i.e., $\chi \propto (T + \Delta)^{-1}$. The induced magnetic form factor has also been measured in $Ce_{0.74}Th_{0.26}$ and in TmSe, and it is found to correspond to that expected for simple atomic $Ce^{3+}(4f^1)$ and $Tm^{3+}(4f^{12})$ even though both of these materials are in mixed-valence phases.[24,25] In a

homogeneous model for the mixed-valence phase, the ground-state wave function would be a hybridization of those appropriate of $4f^6$ and $4f^5 5d$ and in calculating the magnetic moment there would be cross terms which alter the moment and form factor.

### B. Phase diagram

There are two aspects to the phase diagram: one is the detailed shape of the phase boundary in the $P$-$T$ plane for pure SmS and the second is whether the transition is discontinuous or continuous as substitutions are made either for the Sm as in $Sm_{1-x}Y_xS$ or for the chalcogen as in $SmS_{1-x}Se$ or SmSe and SmTe. The lattice-parameter measurements have a bearing on the first aspect.

The slope of the phase boundary is related to the entropy change $\Delta S$ and the volume change $\Delta V$ at the transition by the Clapeyron equation:

$$\frac{dP}{dT} = \frac{\Delta S}{\Delta V} = \frac{S_{met} - S_{ins}}{V_{met} - V_{ins}} .$$

If the volume change (taken from Fig. 1) is assumed to be independent of temperature, then $\Delta S$ can be calculated from the observed slope of the phase boundary. (The data in Fig. 1 given no evidence for a substantial change in $\Delta V$ between 85 and 298 K.) The early resistivity measurements made at 4.2 and 473 K suggested that the phase boundary had a negative slope, and an estimate of the entropy change at the transition of $S_{met}$-$S_{ins} = 0.2R$ was made.[8] Subsequently, differential thermal analysis and further resistivity measurements at higher temperatures established that $dT/dP$ was positive (and $\Delta S < 0$) at and above 298 K.[26] The present hydrostatic measurements confirm that $dT/dP$ is negative below room temperature and that the phase boundary is reentrant. There is a large hysteresis in this first-order transition, so that the equilibrium phase boundary is difficult to establish. The hysteresis loop could become larger at low temperatures, but as the phase boundary as a function of $x$ is reentrant in $Sm_{1-x}Gd_xS$, the equilibrium boundary for SmS might be expected to be similar. A reentrant phase boundary is possible for a pressure-induced insulator to metal transition because at low temperature the electronic entropy of the metallic phase dominates while at higher temperatures the larger lattice entropy of the insulating phase, with its larger volume, may dominate. In the case of SmS there are contributions from the thermal population of the spin-orbit or crystal-field multiplets of the localized $4f$ electrons. The experimental $\Delta S$ curve can be used in conjunction with thermodynamic arguments to estimate the electronic entropy in the mixed-valence phase.

The phase diagram and entropy change are shown in Fig. 4. The data points for the phase boundary with increasing pressure at different temperatures are from resistivity, differential thermal analysis, and neutron diffraction measurements. Using the Clapeyron equation and a constant volume change at the transition of $\Delta V = -4.1$ cm$^3$mole$^{-1}$, the entropy change at the transition can be calculated in the temperature range $200 < T < 460$ K. These values of $\Delta S$ and those obtained directly from the heat capacity in the temperature range below $T = 20$ K are shown as the solid portions of the $\Delta S_{exp}$ curve at the bottom of Fig. 4. The dashed portion of the curve represents a smooth interpolation between 20 and 200 K which is consistent with the observed shift in

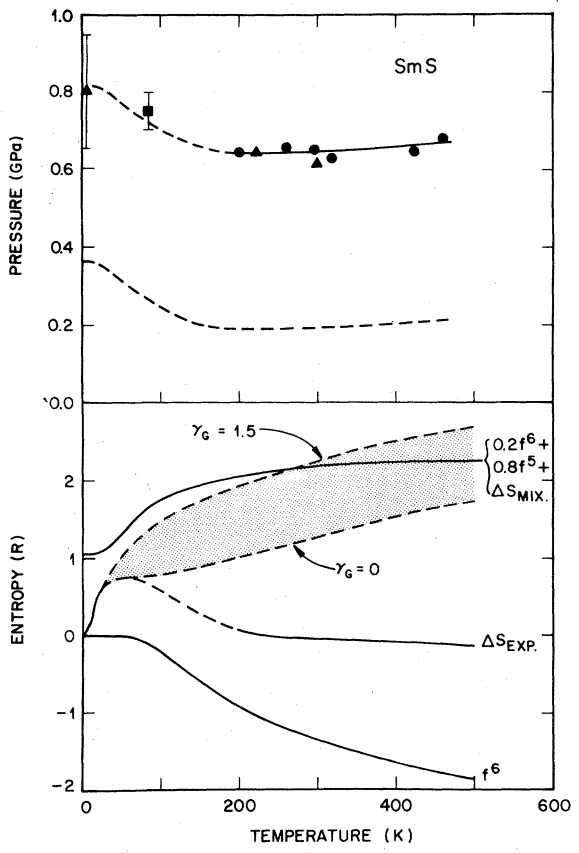


FIG. 4. Phase diagram (top) and entropy (bottom) vs temperature for SmS. The data points are from Ref. 7 (triangles and circles), Ref. 8 (diamonds), and present work (squares). The electronic entropy in the mixed-valence phase is shown as a band at high temperatures representing two limits of the lattice contribution to $\Delta S$ at the transition. The solid line at the top of the entropy curves represents the electronic entropy based on an ionic model of $0.2(4f^6) + 0.8(4f^5) + \Delta S_{mix.}$

the transition pressure at low temperatures. The dashed portion of the phase boundary represents an integration of the $\Delta S_{exp}$ curve. Finally the phase boundary for decreasing pressure is sketched schematically and its position is estimated from the measured value at room temperature.

The entropy change at the transition is composed of contributions from the electronic and lattice entropies of each phase.

$$S_{met} - S_{ins} = \Delta S_{latt} + S_m[0.8(4f^5 5d) + 0.2(4f^6)] - S_I(4f^6).$$

The last term arises from the thermal population of the $J = 0, 1, \ldots, 6$ levels of the $^7F_n$ multiplet, and it can be calculated using the experimental value of $E(^7F_1)$-$E(^7F_0) = 420$ K and the Landé interval rule. This contribution $[-S_I(4f^6)]$ is shown as the bottom curve in Fig. 4. In order to obtain a curve of $S_m$ vs $T$ it is necessary to estimate $\Delta S_{latt}$. For the vast majority of materials, the average phonon density of states varies inversely as the volume, and typical values of the Grüneisen parameters ($\gamma_G = -d\ln\Theta_D/d\ln V$) are $\gamma_G = 1$–$1.5$. If this is true for an isostructural first-order phase transition, then the lattice contribution to the entropy is less than zero, $\Delta S_{latt} = S_{met} - S_{ins} < 0$. It is known that in the alloy system $Sm_{1-x}Y_xS$ the bulk modulus and some of the long-wavelength acoustical phonons go soft as a function of $x$ on the metallic side near the transition.[27] This led some authors to estimate $\Delta S_{latt}$ using a continuum model and to note that $\Delta S_{latt} \geq 0$ is consistent with the available data.[28] It is difficult to believe that the overall phonon density of states will not shift to higher frequencies with the large volume contraction at the transition. Two reasonable limits for $\Delta S_{latt}$ are (i) no change in lattice entropy ($\gamma_G = 0$) and (ii) a Debye model estimate for the lattice term with $\gamma_G = 1.5$, $\Theta_D$(insulator) = 273 K, and $\Theta_D$(metal) = 323 K. The estimate of the electronic entropy in the mixed-valence phase which results from combining these terms ($S_m = \Delta S_{exp} - \Delta S_{latt} + S_{ins}$) is shown as a band in the bottom half of Fig. 4.

The electronic entropy of the mixed-valence phase varies at $\gamma T$ at low temperature and then saturates at a value near $2R$ at higher temperatures. This is the qualitative behavior expected for a heavy Fermi liquid, and it should be compared at high temperatures with the entropy of a random mixture of 0.8 $4f^5$ ions and 0.2 $4f^6$ ions. In the limit where the 0.2 $4f$ electrons diffuse through the lattice as in a classical liquid, there would be an additional translational entropy of $0.2 \times (\frac{3}{2})R$, and finally there is a small $\gamma T$ term resulting from the 0.8 $5d$ electrons. The entropy of the static random mixture can be calculated assuming the crystal field and multiplet energy levels discussed above, and the resulting curve is shown in Fig. 4. This curve is in the experimental range obtained above, and the addition of the contributions from the motion of the 0.8 $5d$ and 0.2 $4f$ electrons would raise the curve only (0.2–0.3)$R$. One concludes that the electronic entropy of the mixed-valence phase obtained from the low-temperature heat capacity and from the phase diagram are consistent with the model of a continuous transition from a heavy Fermi liquid to a classical liquid with increasing temperature.

## IV. SUMMARY

Elastic- and inelastic-neutron-scattering studies have been presented which show that a fundamental change in the electronic structure at the atomic level occurs at the transition at 6.5 GPa. There are no observable changes from an ionic description of $Sm^{2+}$ $4f^6$ ions right up to the transition. In the mixed-valence phase above 6.5 GPa there is no evidence for sharp excitations corresponding to magnetic dipole transitions between normal crystal field or spin-orbit levels. These results and the estimated electronic entropy of the mixed-valence phase are consistent with the model of a two-component Fermi liquid.

## ACKNOWLEDGMENTS

We thank E. Bucher, G. Shirane, and C. M. Varma for helpful discussions and A. L. Stevens for technical assistance. Research at Brookhaven National Laboratories was supported by the Division of Basic Energy Sciences, Department of Energy under Contract No. EY-76-C-02-0016. Research at Massachusetts Institute of Technology was supported in part by the NSF.

*Operated by Union Carbide Corp. for the Dept. of Energy.
[1]A. Jayaraman, V. Narayanamurti, E. Bucher, and R. G. Maines, Phys. Rev. Lett. 25, 1430 (1970).
[2]A. Lawson and T. Y. Tang, Phys. Rev. 76, 301 (1949).
[3]H. T. Hall, L. Merrill, and J. D. Barnett, Science 146, 1297 (1964).
[4]D. B. McWhan, T. M. Rice, and J. P. Remeika, Phys. Rev. Lett. 23, 1384 (1969).
[5]M. Marezio, D. B. McWhan, P. D. Dernier, and J. P. Remeika, Phys. Rev. Lett. 28, 1390 (1972).
[6]D. B. McWhan, Science 176, 751 (1972).
[7]A. Chatterjee, A. K. Singh, and A. Jayaraman, Phys. Rev. B 6, 2285 (1975).
[8]S. D. Bader, N. E. Phillips, and D. B. McWhan, Phys. Rev. B 7, 4686 (1973).

[9]M. B. Maple and D. Wohlleben, Phys. Rev. Lett. 27, 511 (1971).
[10]C. M. Varma, Rev. Mod. Phys. L18, 219 (1976); and in *Valence Instabilities and Related Narrow-Band Phenomena*, edited by R. D. Parks (Plenum, New York, 1977), p. 201.
[11]J. M. D. Coey, S. K. Ghatak, and F. Holtzberg, AIP Conf. Proc. 24, 38 (1974).
[12]R. J. Birgeneau, AIP Conf. Proc. 10, 1664 (1973).
[13]S. M. Shapiro, R. J. Girgeneau, and E. Bucher, Phys. Rev. Lett. 34, 470 (1975).
[14]S. M. Shapiro, R. J. Birgeneau, D. B. McWhan, and E. Bucher, Bull. Am. Phys. Soc. 20, 383 (1975).
[15]R. M. Moon, W. C. Koehler, D. B. McWhan, and F. Holtzberg, J. Appl. Phys. 49, 2107 (1978).
[16]J. Eckert, W. B. Daniels, and J. D. Axe, Phys. Rev. B 14, 3649 (1976).
[17]D. B. McWhan and C. Vettier (unpublished).
[18]H. A. Mook, F. W. Snodgrass, and D. D. Bates, Nucl. Instrum. Methods 116, 205 (1974).
[19]K. C. Turberfield, L. Passell, R. J. Birgeneau, and E. Bucher, J. Appl. Phys. 42, 1746 (1971).
[20]W. Marshall and S. W. Lovesey, *Theory of Thermal Neutron Scattering* (Oxford University, London, 1971).
[21]R. J. Birgeneau, J. Phys. Chem. Solids 33, 59 (1972).
[22]S. Methfessel and D. C. Mattis, *Handbuch der Physik, Vol. XVIII/1*, edited by S. Flugge, (Springer-Verlag, Berlin, 1968).
[23]E. Holland-Moritz, M. Loewenhaupt, W. Schmatz, and D. K. Wohlleben, Phys. Rev. Lett. 38, 983 (1977).
[24]S. M. Shapiro, J. D. Axe, R. J. Birgeneau, J. M. Lawrence, and R. D. Parks, Phys. Rev. B 16, 2225 (1977).
[25]H. Bjerrum Moller, S. M. Shapiro, and R. J. Birgeneau, Phys. Rev. Lett. 39, 1021 (1977).
[26]A. Jayaraman, P. D. Dernier, and L. D. Longinotti, Phys. Rev. B 11, 2783 (1975).
[27]R. L. Melcher, G. Guntherodt, T. Penney, and F. Holtzberg, Ultrasonics Symposium Proc. IEEE Cat. 75, CHO 994-4SO, 1975, p. 16.
[28]T. A. Kaplan, S. D. Mahanti, and M. Barma, *Proceedings of the International Conference on High Pressure and Low Temperature Physics* (Plenum, New York, 1978).